Molecular Vision 2013; 19:2312-2320 <http://www.molvis.org/molvis/v19/2312>
Received 31 July 2013 | Accepted 14 November 2013 | Published 16 November 2013

Retinal pigment epithelium protein of 65 kDA gene-linked retinal degeneration is not modulated by chicken acidic leucine-rich epidermal growth factor-like domain containing brain protein/ Neuroglycan C/ chondroitin sulfate proteoglycan 5

Sandra Cottet,[1,2] René Jüttner,[3] Nathalie Voirol,[1] Pierre Chambon,[4] Fritz G. Rathjen,[3] Daniel F. Schorderet,[1,2,5] Pascal Escher[1,2]

[1]Institute for Research in Ophthalmology, Sion, Switzerland; [2]Department of Ophthalmology, University of Lausanne, Lausanne, Switzerland; [3]Max-Delbrück-Centrum, Berlin, Germany; [4]Institut de Génétique et de Biologie Moléculaire et Cellulaire, Collège de France, Strasbourg, France; [5]EPFL-Ecole Polytechnique Fédérale, Lausanne, Switzerland

Purpose: To analyze in vivo the function of chicken acidic leucine-rich epidermal growth factor-like domain containing brain protein/Neuroglycan C (gene symbol: Cspg5) during retinal degeneration in the *Rpe65*$^{-/-}$ mouse model of Leber congenital amaurosis.

Methods: We resorted to mice with targeted deletions in the *Cspg5* and retinal pigment epithelium protein of 65 kDa (*Rpe65*) genes (*Cspg5*$^{-/-}$/*Rpe65*$^{-/-}$). Cone degeneration was assessed with cone-specific peanut agglutinin staining. Transcriptional expression of rhodopsin (*Rho*), S-opsin (*Opn1sw*), M-opsin (*Opn1mw*), rod transducin α subunit (*Gnat1*), and cone transducin α subunit (*Gnat2*) genes was assessed with quantitative PCR from 2 weeks to 12 months. The retinal pigment epithelium (RPE) was analyzed at P14 with immunodetection of the retinol-binding protein membrane receptor Stra6.

Results: No differences in the progression of retinal degeneration were observed between the *Rpe65*$^{-/-}$ and *Cspg5*$^{-/-}$/*Rpe65*$^{-/-}$ mice. No retinal phenotype was detected in the late postnatal and adult *Cspg5*$^{-/-}$ mice, when compared to the wild-type mice.

Conclusions: Despite the previously reported upregulation of Cspg5 during retinal degeneration in *Rpe65*$^{-/-}$ mice, no protective effect or any involvement of Cspg5 in disease progression was identified.

Chicken acidic leucine-rich epidermal growth factor-like domain containing brain protein (CALEB)/ Neuroglycan C (NGC), hereafter called chondroitin sulfate proteoglycan 5 (Cspg5) according to its gene symbol, is a transmembrane chondroitin sulfate proteoglycan [1] predominantly expressed at the surfaces of neurons and glial cells in the developing central nervous system [2]. In the mouse, three Cspg5 isoforms generated through alternative exon use and alternative splicing have been described thus far [3–5]. The major Cspg5-I isoform is composed of an N-terminal signal peptide of 30 amino acids (aa) and a 120 kDa core protein (514 aa) formed by five different structural domains: the N-terminal extracellular domain (ECD) containing a chondroitin sulfate attachment site at serine 123 [6], a stretch of acidic amino acids, a single epidermal growth factor (EGF)-like domain embedded in a cysteine-rich domain, a transmembrane region, and a C-terminal cytoplasmic domain [3]. Neuronal depolarization of chick retinal cells facilitated the processing of full-length Cspg5 into a truncated transmembrane form and an ectodomain, thus exposing the EGF-like domain [7]. A recombinant ectodomain promoted neurite outgrowth from rat neocortical neurons [8], and the EGF-like domain alone mediated the dendritic tree and spine complexity in primary hippocampal neurons and, in vivo, in the electroporated embryonic mouse cortex [9]. Cspg5 was also recently shown to be necessary for the proper radial migration of neurons in the developing mouse cerebral cortex [10].

Mice with a targeted disruption of the *Cspg5* gene (*Cspg5*$^{-/-}$ mice) were morphologically normal, viable, and fertile, but with decreased maternal behavior [7]. Electrophysiological analyses showed several distinct abnormalities at early postnatal stages (P1–P3), but not at P20–P22: higher paired-pulse ratios, less depression during prolonged repetitive activation, a lower rate of spontaneous synaptic currents, and a lower release probability at gamma-aminobutyric acid (GABA)ergic synapses [7]. The retina appeared morphologically normal in the *Cspg5*$^{-/-}$ mice [7]. Retinal Cspg5 expression was reduced at the late postnatal and the adult stages (P14–P42), when synapse maturation was complete [11]. In

Correspondence to: Pascal Escher, IRO-Institut de Recherche en Ophtalmologie Grand-Champsec 64, CH-1950 Sion, Switzerland; Phone: ++41 (0)27 205 79 02; FAX: ++41 (0)27 205 79 01; email: pascal.escher@irovision.ch

the retinal pigment epithelium (RPE), Cspg5 was differentially expressed during development [11]. At P7, Cspg5 was localized to the basal infoldings of the RPE cells, facing the choroid. In the adult, Cspg5 was expressed at the highest levels at the microvilli of the apical surface, facing the neural retina [5,11].

We previously reported increased Cspg5 mRNA and protein expression in the retina and the RPE of *Rpe65*$^{-/-}$ mice, an animal model of Leber congenital amaurosis (LCA), during disease progression [5,12]. Retinal pigment epithelium protein of 65 kDa (RPE65) is the iron(II)-dependent isomerohydrolase essential for generating the photopigment 11-cis retinal from all-trans-retinyl ester in the retinoid visual cycle [13,14]. The lack of 11-cis retinal in *Rpe65*$^{-/-}$ mice resulted in cone photoreceptor degeneration with cone opsin mislocalization to the inner segment within the first postnatal weeks and a concomitant decrease in cone-specific gene expression [12,15]. In contrast, rod photoreceptor degeneration progressed slowly, dependent on residual transduction cascade by unliganded opsin [16], and rhodopsin remained correctly localized in aged animals [17–19]. To further investigate whether Cspg5 upregulation may exert a protective effect against retinal degeneration in the absence of RPE65, we analyzed cone and rod photoreceptor survival in wild-type, *Cspg5*$^{-/-}$, *Rpe65*$^{-/-}$, and *Cspg5*$^{-/-}$*/Rpe65*$^{-/-}$ mice, with the working hypothesis that enhanced progression of retinal degeneration in *Cspg5*$^{-/-}$*/Rpe65*$^{-/-}$ mice might be observed.

METHODS

Animal handling: All experiments performed in this study were in accordance with the Association for Research in Vision and Ophthalmology (ARVO) Statement for the Use of Animals in Ophthalmic and Vision Research and were approved by the Veterinary Service of the State of Valais (Switzerland). Mice were kept in a 12 h:12 h light-dark cycle with unlimited access to food and water. *Rpe65*$^{-/-}$ mice [17] and *Cspg5*$^{-/-}$ mice [7] had been backcrossed in a C57BL/6J genetic background. For genotyping *Rpe65*$^{-/-}$ mice, primers RPE65_WT_F (5′-TCA TGG TCT AGC CAT GTC TG-3′) and RPE65_Com_R (5′-AAT CCC TAC CAG ATG CCA TC-3′) were used to amplify a 155 bp fragment in intron 3 of the wild-type allele, downstream of the targeted exon 3. To detect the targeted allele, primers RPE65_KO_F (5′-CAC TTG TGT AGC GCC AAG TG-3′), located in the human phosphoglycerate kinase promoter (PGK), and RPE65_Com_R were used to amplify a fragment of about 200 bp. *Cspg5*$^{-/-}$ mice were genotyped as previously described [7]. We used C57BL/6J mice as the wild-type controls (RCC, Basel, Switzerland).

Ribonucleic acid preparation and quantitative polymerase chain reaction: RNA from mouse retinas and pure RPE cells was prepared and analyzed with quantitative PCR as previously described [5]. Mice were killed by cervical dislocation. Eyes were enucleated, immobilized with 0.2 mm Austerlitz insect pins (Fine Science Tools, Heidelberg, Germany) on a Sylgard 184-filled cell culture dish (Dow Corning, Midland, MI) and covered with 1x PBS (phosphate-buffered saline: 154 mM NaCl, 1 mM KH_2PO_4, 3 mM Na_2HPO_4 heptahydrate). The eyeball was sectioned below the ora serrata to remove cornea, lens, iris and other attached tissues. The retina was detached from the pigmented epithelium (RPE) and then homogenized with 18G Sterican needles (Braun, Melsungen, Germany) in TRI Reagent® (Molecular Research Center Inc., Cincinnati, OH). Pure RPE cells were obtained by digesting the posterior eyecup comprised of RPE, choriocapillaris, and sclera in 0.2% trypsin (Invitrogen, Basel, Switzerland) for 1 h at 37 °C in a 5% CO_2 atmosphere. RPE cells were gently peeled off with forceps and transferred into TRI Reagent®. Total RNA was prepared according to manufacturer's instructions, with prolonged centrifugation times to increase RNA recovery. Reverse transcription was performed on 500 ng of total RNA (1st strand cDNA synthesis kit for RT–PCR (AMV); Roche, Basel, Switzerland). Quantitative PCR was performed on an Mx3000p sequence analyzer using Fast Start Universal SYBR®Green Master Mix (Roche). Experimental data points with cycle threshold (Ct) values above 30 were not considered for data analysis. Expression of the ribosomal protein L8 (RL8) was used as internal standard. Primers are listed in Table 1.

Immunohistochemistry: Eyes were enucleated and fixed in 4% paraformaldehyde-1X PBS for 2 h at 4 °C. After cryoprotection by immersion in 30% sucrose-1x PBS overnight at 4 °C, eyes were embedded in freezing compound (30% albumin/3% gelatine in 1X PBS). For immunohistochemistry, 12-mm cryosections were collected on Superfrost®Plus glass slides (Menzel Gläser, Braunschweig, Germany). Sections were dried at room temperature for at least 1 h, quickly hydrated with 1X PBS and blocked for 1 h in 1X PBS containing 2% goat serum and 0.2% Triton X-100. A rabbit polyclonal serum raised against amino acids 565–670 of Stra6 was diluted at 1:200 in blocking solution and incubated overnight at 4 °C [20]. Sections were then briefly rinsed twice with blocking solution and washed once for 5 min. A secondary anti-rabbit antibody conjugated to Alexa Fluor 594 (Molecular Probes, Invitrogen, Eugene, OR) was diluted at 1:1,000 and incubated for 1 h at room temperature in the dark. Sections were rinsed briefly twice in 1X PBS and then washed three times for 5 min. To visualize nuclei, sections were stained in 300 nM 4'-6-diamidino-2-phenylindole

Table 1. Primers for quantitative PCR

Gene (mus)	Forward primer (5′-3′)	Reverse primer (5′-3′)	GenBank accession number	Location (nt)
Abca4	ATCGAGGAGTACTCAGTCAC	CCTGGTGTGCTTATCTTCTG	NM_007378	6775–7008
Gnat1	AGAGGATGCTGAGAAGGATG	ACTGAATGTTGAGCGTGGTC	NM_008140	104- 315
Gnat2	CATCAGTGCTGAGGACAAAG	GACTTGAACTCTAGGCACTC	NM_008141	93- 294
Impg1	AATCGAAAGCTACTCCCTCG	TTGTAGAGTGATCTGGTGGC	NM_022016	2084–2332
Impg2	CTTCTGCTGTCGTCTTCTTC	CCAATCACCTCTTCACTAGC	BC048863	3544–3769
Lrat	AGCCTACTGTGGAACAACTG	CAGACATCATCCACAAGCAG	NM_023624	724- 953
Cspg5	GACTGAGAATACCAAGCTGC	TTGGGTGACATGGAGTTCTG	NM_013884	1500–1700
Opn1mw	TGAGGATAGCACCCATGCAA	GGCGCAGCTTCTTGAATCTC	NM_008106	83- 282
Opn1sw	TGGTCAACAATCGGAACCAC	AGGGCCAACTTTGCTAGAAG	NM_007538	874–1100
Rbp1	AATCGCCAACTTGCTGAAGC	TCTGCACACACTGGAGTTTG	X60367	2113–2312
Rbp3	TACTTCTTTGACGAGGCACC	CTTGTCACTTCACCGATGAC	NM_015745	3361–3584
Rdh5	TACCTCCAGCTATACAGGCC	ATCCAGGTGAGCACAGCATC	NM_134006	867–1107
Rdh12	TCACTCGAGAACTGGCTAAG	TGACGTTCCACAATCGCTCA	NM_030017	756–1046
Rho	CTCCATGCTGGCAGCGTACA	TGCTCATCGGCTTGCAGACC	NM_145383	189- 511
RL8	ACTGGACAGTTCGTGTACTG	GCTTCACTCGAGTCTTCTTG	NM_012053	271- 469
Stra6	GCTACTCCGAGAAGTATCTG	TTCTGCACAGTAGGCACCAC	AF062476	1083–1323

The location of the PCR amplification products is indicated with respect to nucleotide numbering of the indicated GenBank accession numbers.

dichloride (DAPI; Sigma-Fluka, Buchs, Switzerland) for 20 min at room temperature. Slides were washed three times for 5 min in 1X PBS, before mounting in Cityfluor AF3 (Cityfluor, London, England). To assess cone degeneration, slides were first stained with DAPI, and then cone photoreceptor outer segments were stained with 20 µg/ml fluorescein-conjugated peanut agglutinin (FITC-PNA; Sigma-Fluka) for 75 min at room temperature and rinsed 3 times for 5 min in 1X PBS, before mounting in Cityfluor AF3.

Cone photoreceptor counting: FITC-PNA-stained sections were analyzed with an Olympus BX61 fluorescent microscope equipped with a digital DP71 camera (Olympus, Volketswil, Switzerland). For each genotype, 9–12 micrographs from three eyes were taken at a 200X magnification, and the labeled cones present in the field of view counted. Images were processed with Adobe Photoshop 7 (Adobe Systems, Mountain View, CA) to overlay the FITC-PNA and DAPI staining.

Statistical analysis: The cone photoreceptor counting data presented in Figure 1 were analyzed with the Student *t* test, after testing for equal variances and normal distribution. Quantitative PCR data presented were analyzed with two-way ANOVA, using factors of genotype and age (Prism 4.0.2; GraphPad Software, La Jolla, CA).

RESULTS

No alteration in retina- and retinal pigment epithelium-specific gene expression in Cspg5$^{-/-}$ mice: To assess retinal gene expression in mutant mice, quantitative PCR analysis was performed in 2-month-old wild-type and *Cspg5$^{-/-}$* mice. No altered mRNA expression of the phototransduction (*Rho, Opn1mw, Opn1sw*), the visual cycle (*Rbp1, Rbp3, Abca4, Stra6, Lrat, Rdh5, Rdh12*) and the interphotoreceptor matrix (IPM; *Impg1, Impg2*) genes was observed in the retina and the RPE of *Cspg5$^{-/-}$* mice (Table 2).

Cone degeneration progresses similarly in Rpe65$^{-/-}$ and *Cspg5$^{-/-}$/Rpe65$^{-/-}$* mice: Cone degeneration in the central retina appeared to progress similarly in *Rpe65$^{-/-}$* and *Cspg5$^{-/-}$/Rpe65$^{-/-}$* mice, and the *Cspg5$^{-/-}$* mouse was comparable to that of the wild-type (Figure 1). At 1 month, when the cones had almost disappeared in the central retina of the *Rpe65$^{-/-}$* and *Cspg5$^{-/-}$/Rpe65$^{-/-}$* mice, some cones were still present in the periphery. When the mice were 2 months old, almost no cones were present in *Rpe65$^{-/-}$* (Figure 2C) and *Cspg5$^{-/-}$/Rpe65$^{-/-}$* mice (Figure 2D), while prominent staining of cone outer segments was observed in the central retina of the wild-type (Figure 2A) and *Cspg5$^{-/-}$* mice (Figure 2B). In the periphery of the *Cspg5$^{-/-}$/Rpe65$^{-/-}$* retinas, residual staining of cones was still observed, with mislocalized labeling in the inner

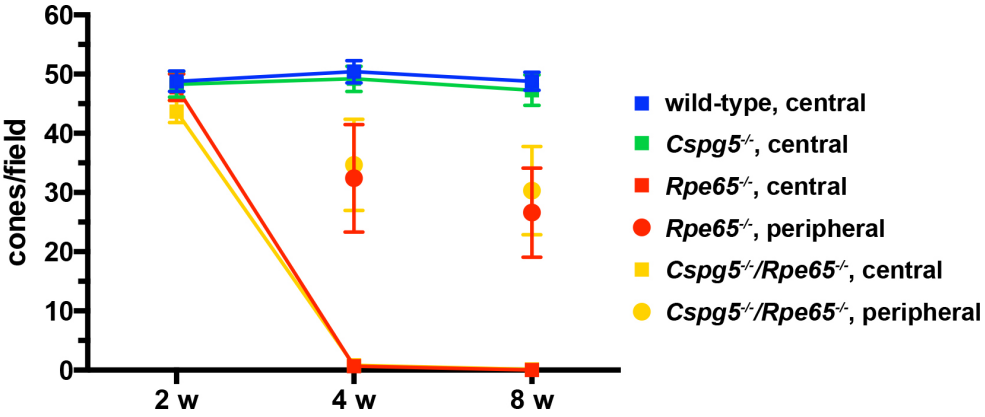

Figure 1. Progression of cone degeneration in retinal pigment epithelium protein of 65 kDa (*Rpe65*)$^{-/-}$ and *Cspg5*$^{-/-}$/*Rpe65*$^{-/-}$ retinas. Fluorescein-conjugated peanut agglutinin (FITC-PNA)-labeled cones were counted on retinal sections of 2-, 4-, and 8-week-old mice. Cones had almost disappeared in the central retina of the 4- and 8-week-old *Rpe65*$^{-/-}$ and *Cspg5*$^{-/-}$/*Rpe65*$^{-/-}$ mice. The peripheral region considered for cone counting in the *Rpe65*$^{-/-}$ and *Cspg5*$^{-/-}$/*Rpe65*$^{-/-}$ mice was located toward the edges of the retina. With two-way ANOVA using factors of genotype and age, no significant differences were found between the *Rpe65*$^{-/-}$ and *Cspg5*$^{-/-}$/*Rpe65*$^{-/-}$ mice in the number of cones, in the central and peripheral retina (n=4). For all time points, the number of cones per field of view±standard error of the mean (SEM) is shown.

segments and at the synaptic endfeet of cone photoreceptors (Figure 2E).

Cone-specific gene expression declines similarly in Rpe65$^{-/-}$ and *Cspg5*$^{-/-}$/*Rpe65*$^{-/-}$ mice: The expression of cone-specific *Opn1mw*, *Opn1sw*, and *Gnat2* genes was assessed with quantitative PCR from 2 weeks to 6 months of age in wild-type, *Cspg5*$^{-/-}$, *Rpe65*$^{-/-}$, and *Cspg5*$^{-/-}$/*Rpe65*$^{-/-}$ mice (Figure 3). No significant changes in mRNA expression were observed between the wild-type and *Cspg5*$^{-/-}$ retinas. Transcript levels decreased similarly in the *Rpe65*$^{-/-}$ and *Cspg5*$^{-/-}$/*Rpe65*$^{-/-}$ retinas, to reach at 6 months about 30% and 25% of the wild-type levels for *Opn1mw* and *Gnat2*, respectively. The *Opn1sw* levels were at the limit of detection from 2 months on.

Rod-specific gene expression during retinal degeneration: The expression of rod-specific *Rho* and *Gnat1* genes was assessed with quantitative PCR from 2 weeks to 12 months of age in the wild-type, *Cspg5*$^{-/-}$, *Rpe65*$^{-/-}$, and *Cspg5*$^{-/-}$/*Rpe65*$^{-/-}$ mice (Figure 4). The *Rho* and *Gnat1* levels slowly decreased between 2 and 12 months by about 30% in the *Rpe65*$^{-/-}$ and *Cspg5*$^{-/-}$/*Rpe65*$^{-/-}$ retinas, compared to the wild-type and *Cspg5*$^{-/-}$ retinas. However, no difference in *Rho* and *Gnat1*

Table 2. Gene expression in retina and RPE of *Cspg5*$^{-/-}$ mice

Gene	Retina 2 month		RPE 2 month	
	wild-type	Cspg5$^{-/-}$	wild-type	Cspg5$^{-/-}$
Abca4	1.00±0.14	1.08±0.06	n.t.	n.t.
Impg1	1.00±0.05	1.09±0.06	1.00±0.05	1.00±0.05
Impg2	1.00±0.11	1.11±0.18	1.00±0.06	0.96±0.03
Lrat	1.00±0.04	1.02±0.09	1.00±0.09	1.13±0.14
Cspg5	1.00±0.09	n.d.	1.00±0.03	n.d.
Opn1mw	1.00±0.04	0.97±0.08	n.t.	n.t.
Opn1sw	1.00±0.18	0.92±0.06	n.t.	n.t.
Rbp1	1.00±0.04	1.03±0.07	1.00±0.15	1.11±0.04
Rbp3	1.00±0.12	1.07±0.05	1.00±0.10	0.99±0.04
Rdh5	n.t.	n.t.	1.00±0.16	1.15±0.07
Rdh12	1.00±0.07	1.15±0.17	1.00±0.04	0.97±0.03
Rho	1.00±0.07	1.08±0.04	n.t.	n.t.
Stra6	1.00±0.11	1.15±0.05	1.00±0.11	1.18±0.08

Quantitative PCR was performed with primers listed in Table 1. Normalized data from 4 different mice±standard deviation are shown. n.d.: not detected; n.t.: not tested

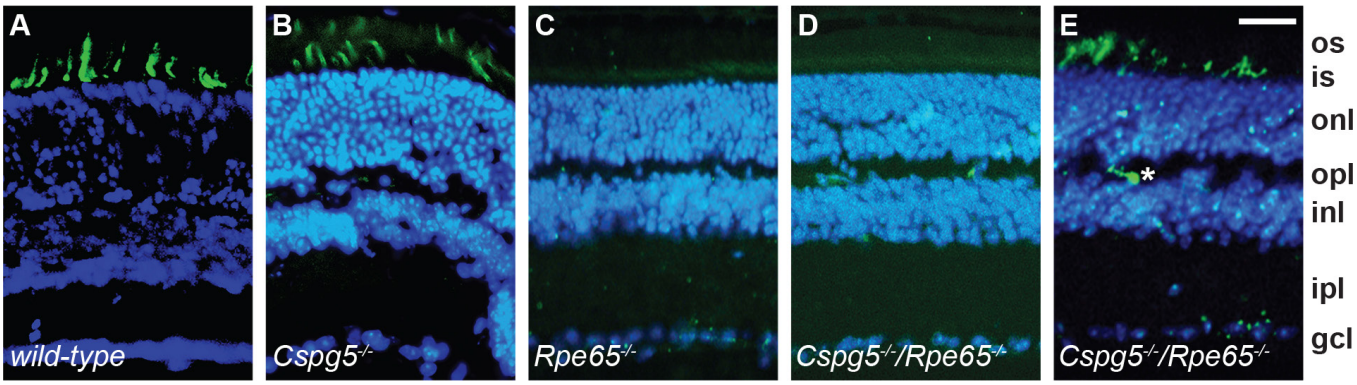

Figure 2. Cone degeneration in *Rpe65*$^{-/-}$ and *Cspg5*$^{-/-}$/*Rpe65*$^{-/-}$ retinas. Central regions of retinas from 8-week-old wild-type (**A**), *Cspg5*$^{-/-}$ (**B**), *Rpe65*$^{-/-}$, and (**C**) *Cspg5*$^{-/-}$/*Rpe65*$^{-/-}$ (**D**) mice were analyzed. Cones were labeled with fluorescein-conjugated peanut agglutinin (green), nuclei were stained with 4',6-diamidino-2-phenylindole dihydrochloride (blue), and the images were merged. The cone outer segments were prominently stained in the wild-type and *Cspg5*$^{-/-}$ retinas (A, B). Residual staining of cone inner segments was observed in the central retina of the *Rpe65*$^{-/-}$ and *Cspg5*$^{-/-}$/*Rpe65*$^{-/-}$ mice (**C**, **D**). In the peripheral regions of the *Cspg5*$^{-/-}$/*Rpe65*$^{-/-}$ retinas, cone outer segment labeling was still observed, with mislocalization to the synaptic endfeet of cone photoreceptors (star; **E**). Abbreviations: photoreceptor outer segments (os); photoreceptor inner segments (is); outer nuclear layer (onl); outer plexiform layer (opl); inner nuclear layer (inl); inner plexiform layer (ipl); ganglion cell layer (gcl). Scale bar equals 50 µm.

expression was observed in the *Cspg5*$^{-/-}$/*Rpe65*$^{-/-}$ retinas compared to the *Rpe65*$^{-/-}$ retinas.

Preservation of the retinal pigment epithelium in Cspg5$^{-/-}$ and *Cspg5*$^{-/-}$/*Rpe65*$^{-/-}$ retinas: During early postnatal development, Cspg5 protein is predominantly expressed on the basal side of the RPE [11]. The retinol-binding protein membrane receptor Stra6, mediating the cellular uptake of vitamin A in the RPE, is also located at the basolateral membrane of the RPE [21]. To further investigate the integrity of the RPE in the absence of Cspg5, immunohistochemical analysis was performed to detect Stra6 protein in P14 wild-type, *Cspg5*$^{-/-}$, *Rpe65*$^{-/-}$, and *Cspg5*$^{-/-}$/*Rpe65*$^{-/-}$ mice (Figure 5). Stra6 was predominantly localized at the basolateral membrane of the

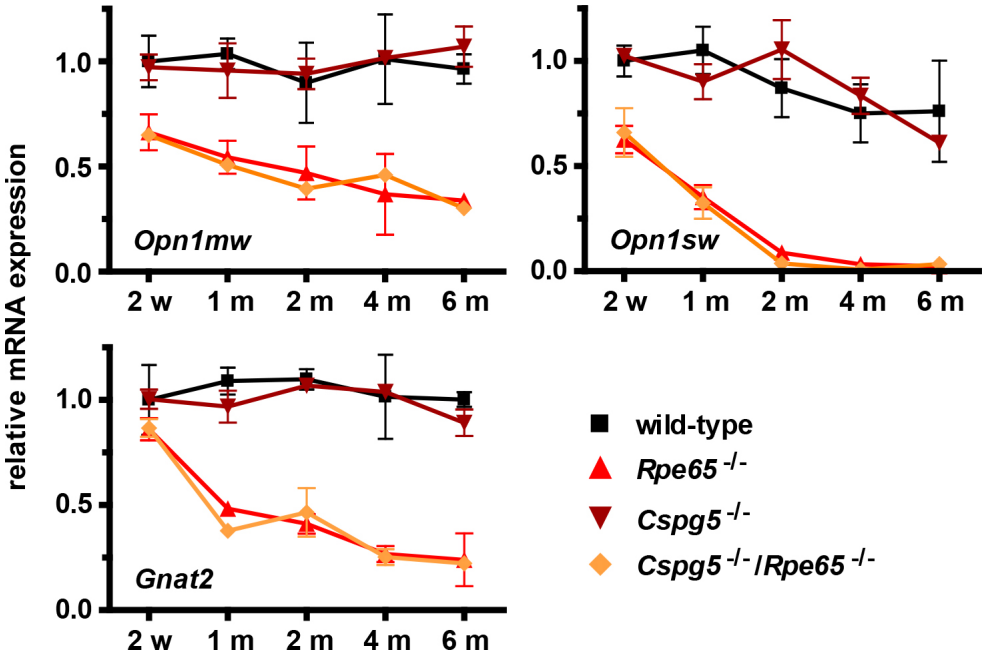

Figure 3. Time-course of cone-specific gene expression. The expression of the cone-specific M-opsin (*Opn1mw*), S-opsin (*Opn1sw*), and cone transducin alpha subunit (*Gnat2*) genes was assessed with quantitative PCR. Total RNA was extracted from the retinas of the wild-type, *Rpe65*$^{-/-}$, *Cspg5*$^{-/-}$, and *Cspg5*$^{-/-}$/*Rpe65*$^{-/-}$ mice at ages 2 weeks (w) to 6 months (m). For each time point and genotype, three animals were analyzed in duplicate. Wild-type retinal mRNA expression was arbitrarily set to 1 at 2 weeks. For all panels, fold inductions±standard error of the mean (SEM) are shown. With two-way ANOVA, using factors of time and genotypes, no significant changes in relative mRNA expression between the wild-type and *Cspg5*$^{-/-}$ mice, and between *Rpe65*$^{-/-}$ and *Cspg5*$^{-/-}$/*Rpe65*$^{-/-}$ mice were detected.

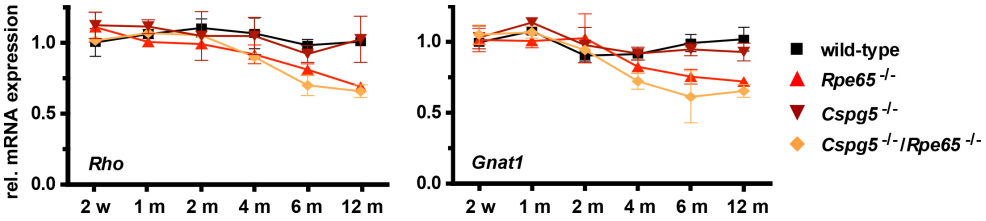

Figure 4. Time-course of rod-specific gene expression. Total RNA was extracted from the retinas of the wild-type, *Rpe65*$^{-/-}$, *Cspg5*$^{-/-}$, and *Cspg5*$^{-/-}$/*Rpe65*$^{-/-}$ mice at ages 2 weeks (w) to 12 months (m). Rhodopsin (*Rho)* and rod transducin alpha subunit (*Gnat1*) gene expression was assessed with quantitative PCR, with four animals analyzed in duplicate for each genotype. Wild-type mRNA expression was arbitrarily set to 1 at 2 weeks. For all panels, fold inductions±standard error of the mean (SEM) are shown. With two-way ANOVA, no significant changes in relative mRNA expression between wild-type and *Cspg5*$^{-/-}$ mice, and between *Rpe65*$^{-/-}$ and *Cspg5*$^{-/-}$/*Rpe65*$^{-/-}$ mice were detected during progression of the disease.

RPE in all mouse genotypes, suggesting that the absence of Cspg5 expression did not alter the integrity of the RPE.

DISCUSSION

The loss of photoreceptors in the outer retina is accompanied by morphological and biochemical alterations including a decrease in the IPM, modification of the extracellular matrix as well as impaired intercellular interactions susceptible to

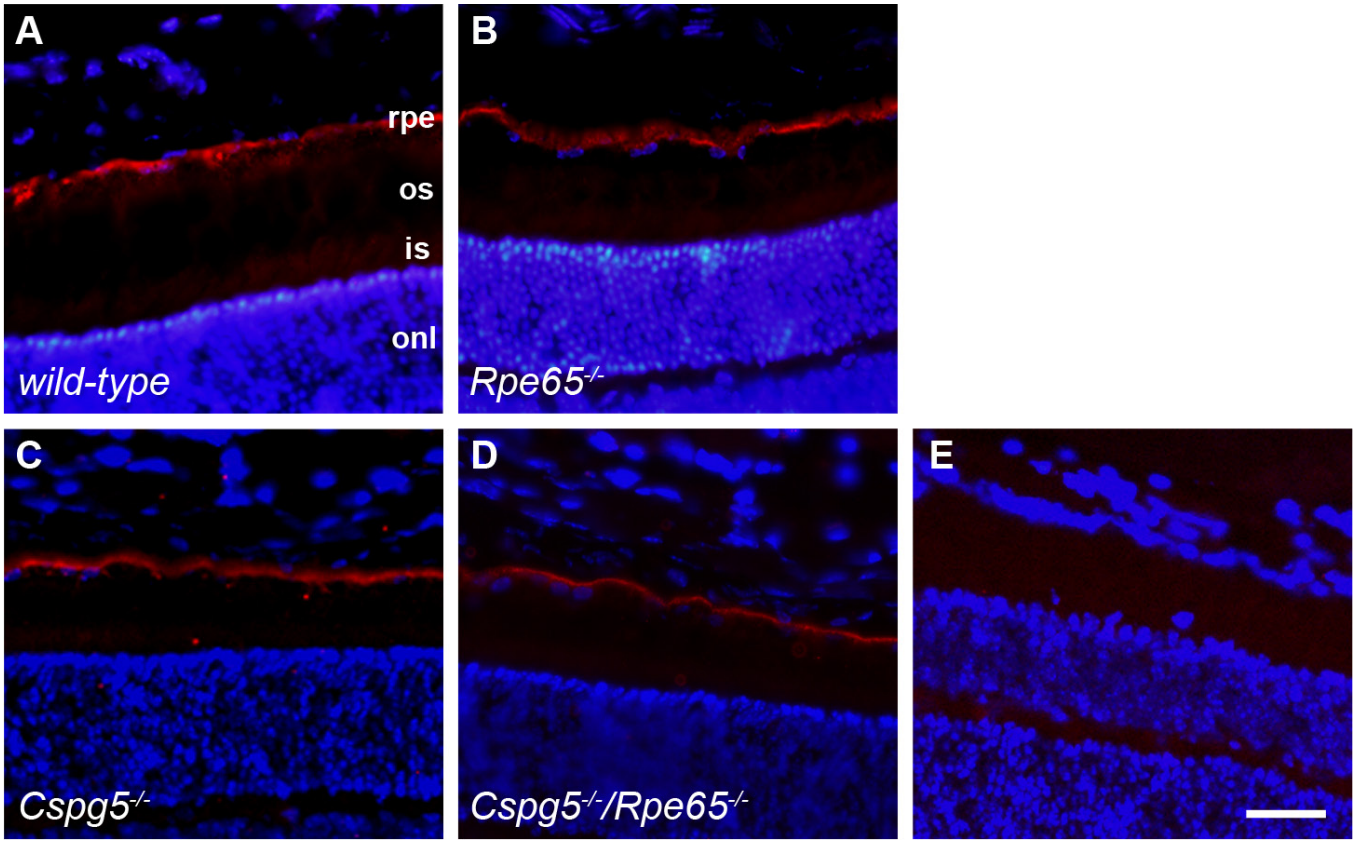

Figure 5. Stra6 protein expression in the P14 mouse retina. Immunohistochemical analysis was performed with a rabbit polyclonal serum raised against the C-terminus of Stra6 (red), on retinal sections of wild-type (**A**), *Rpe65*$^{-/-}$ (**B**), *Cspg5*$^{-/-}$, and (**C**) *Cspg5*$^{-/-}$/*Rpe65*$^{-/-}$ (**D**) mice. Stra6 was predominantly expressed at the basolateral membrane of the retinal pigment epithelium (RPE) in all analyzed genotypes. The nuclei were stained in blue with 4',6-diamidino-2-phenylindole dihydrochloride (DAPI), and the images were merged. As a negative control, a serum of a non-immunized rabbit was used, the nuclei stained with DAPI, and the images merged (**E**). Abbreviations: retinal pigment epithelium (rpe); photoreceptor outer segments (os); photoreceptor inner segments (is); outer nuclear layer (onl). Scale bar equals 40 µm.

influence retinal pathogenesis [22,23]. Several reports have described altered levels of proteoglycans in the IPM and the apical surface of the RPE in rodent models of retinal degeneration including light-induced, rd1, and *Rho*$^{-/-}$ mice and Royal College of Surgeon (RCS) rats [24–27]. In addition, disruption of IPM proteoglycans following intravitreal injection of xyloside, an inhibitor of chondroitin sulfate proteoglycans, has been shown to trigger cone outer segment degeneration and retinal detachment [28]. Patients with mutations in the retinal interphotoreceptor matrix proteoglycan IMPG2 developed an early-onset form of retinitis pigmentosa [29]. Finally, treatment of RPE cells with chondroitin sulfate resulted in reduced cell density and increased phagocytic activities, suggesting that induced biosynthesis of glycosaminoglycan may affect the metabolic and functional properties of the RPE [30]. Taken together, these observations argue in favor of the role of proteoglycans in maintaining photoreceptor cells.

In the present study, we observed no difference in the progression of cone degeneration in the absence of Cspg5. The early loss of cones in the *Cspg5*$^{-/-}$*/Rpe65*$^{-/-}$ mice was comparable to *Rpe65*$^{-/-}$ mice. Additionally, the observed decrease in rod-specific gene expression during progression of the disease in *Rpe65*$^{-/-}$ mice was not exacerbated in the *Rpe65*$^{-/-}$ mice lacking Cspg5. Altogether, these results indicate that the increased Cspg5 protein observed in the retina of the *Rpe65*$^{-/-}$ mice is not directly involved in the pathogenesis and the progression of retinal degeneration. The results further indicate that Cspg5 does not provide any protective effect on cone and rod photoreceptors survival in *Rpe65*$^{-/-}$ mice. However, our analyses cannot exclude subtle changes, namely, in the retinal architecture and in the development of the retinal synaptic network. Cspg5, originally found in the developing brain, is likely involved in neuritogenesis and synaptogenesis in the central nervous system. Several studies previously reported a role of chondroitin sulfate proteoglycans in regulating neurite outgrowth from retinal cells [31]. High expression of Cspg5 has been described in the nerve fiber and inner plexiform layer during formation of the retinal synapses [7,11]. Moreover, spatiotemporal regulation of Cspg5 has been reported in the developing retina, with decreased expression of the proteoglycan in correlation with maturation of the synapses [11]. In retinal ganglion cells, Cspg5 extensively localized in the spiny budding neurites [11]. These observations argue in favor of a role of Cspg5 in the maturation of the neuronal network during retinogenesis. It therefore suggests that induced expression of Cspg5 in *Rpe65*-deficient retina may reflect a function of the proteoglycan in remodeling the retinal network. More specifically, the high level of the Cspg5 protein in neurite-containing retinal layers may reflect synapse remodeling in response to retinal degeneration in an attempt to maintain proper synaptic transmission in the degenerating *Rpe65*$^{-/-}$ retina.

ACKNOWLEDGMENTS

We thank Dr. T. M. Redmond for the *Rpe65*$^{-/-}$ mice. This work was supported by a grant from Téléthon Action Suisse to PE.

REFERENCES

1. Watanabe E, Maeda N, Matsui F, Kushima Y, Noda M, Oohira A. Neuroglycan C, a novel membrane-spanning chondroitin sulfate proteoglycan that is restricted to the brain. J Biol Chem 1995; 270:26876-82. [PMID: 7592931].
2. Schumacher S, Volkmer H, Buck F, Otto A, Tarnók A, Roth S, Rathjen FG. Chicken acidic leucine-rich EGF-like domain containing brain protein (CALEB), a neural member of the EGF family of differentiation factors, is implicated in neurite formation. J Cell Biol 1997; 136:895-906. [PMID: 9049254].
3. Aono S, Keino H, Ono T, Yasuda Y, Tokita Y, Matsui F, Taniguchi M, Sonta S, Oohira A. Genomic organization and expression pattern of mouse neuroglycan C in the cerebellar development. J Biol Chem 2000; 275:337-42. [PMID: 10617623].
4. Aono S, Tokita Y, Yasuda Y, Hirano K, Yamauchi S, Shuo T, Matsui F, Keino H, Kashiwai A, Kawamura N, Shimada A, Kishikawa M, Asai M, Oohira A. Expression and identification of a new splice variant of neuroglycan C, a transmembrane chondroitin sulfate proteoglycan, in the human brain. J Neurosci Res 2006; 83:110-8. [PMID: 16299773].
5. Escher P, Cottet S, Aono S, Oohira A, Schorderet DF. Differential neuroglycan C expression during retinal degeneration in Rpe65−/− mice. Mol Vis 2008; 14:2126-35. [PMID: 19050768].
6. Aono S, Tokita Y, Shuo T, Yamauchi S, Matsui F, Nakanishi K, Hirano K, Sano M, Oohira A. Glycosylation site for chondroitin sulfate on the neural part-time proteoglycan, neuroglycan C. J Biol Chem 2004; 279:46536-41. [PMID: 15331613].
7. Jüttner R, More MI, Das D, Babich A, Meier J, Henning M, Erdmann B, Müller EC, Otto A, Grantyn R, Rathjen FG. Impaired synapse function during postnatal development in the absence of CALEB, an EGF-like protein processed by neuronal activity. Neuron 2005; 46:233-45. [PMID: 15848802].
8. Nakanishi K, Aono S, Hirano K, Kuroda Y, Ida M, Tokita Y, Matsui F, Oohira A. Identification of neurite outgrowth-promoting domains of neuroglycan C, a brain-specific chondroitin sulfate proteoglycan, and involvement of phosphatidylinositol 3-kinase and protein kinase C signaling pathways in neuritogenesis. J Biol Chem 2006; 281:24970-8. [PMID: 16803884].
9. Brandt N, Franke K, Rasin MR, Baumgart J, Vogt J, Khrulev S, Hassel B, Pohl EE, Sestan N, Nitsch R, Schumacher S. The

neural EGF family member CALEB/NGC mediates dendritic tree and spine complexity. EMBO J 2007; 26:2371-86. [PMID: 17431398].

10. Zhang C, Mejia LA, Huang J, Valnegri P, Bennett EJ, Anckar J, Jahani-Asl A, Gallardo G, Ikeuchi Y, Yamada T, Rudnicki M, Harper JW, Bonni A. The X–Linked Intellectual Disability Protein PHF6 Associates with the PAF1 Complex and Regulates Neuronal Migration in the Mammalian Brain. Neuron 2013; 78:986-93. [PMID: 23791194].
11. Inatani M, Tanihara H, Oohira A, Otori Y, Nishida A, Honjo M, Kido N, Honda Y. Neuroglycan C, a neural tissue-specific transmembrane chondroitin sulfate proteoglycan, in retinal neural network formation. Invest Ophthalmol Vis Sci 2000; 41:4338-46. [PMID: 11095636].
12. Cottet S, Michaut L, Boisset G, Schlecht U, Gehring W, Schorderet DF. Biological characterization of gene response in Rpe65$^{-/-}$ mouse model of Leber's congenital amaurosis during progression of the disease. FASEB J 2006; 20:2036-49. [PMID: 17012256].
13. Jin M, Li S, Moghrabi WN, Sun H, Travis GH. Rpe65 is the retinoid isomerase in bovine retinal pigment epithelium. Cell 2005; 122:449-59. [PMID: 16096063].
14. Moiseyev G, Takahashi Y, Chen Y, Gentleman S, Redmond TM, Crouch RK, Ma JX. RPE65 is an iron(II)-dependent isomerohydrolase in the retinoid visual cycle. J Biol Chem 2006; 281:2835-40. [PMID: 16319067].
15. Znoiko SL, Rohrer B, Lu K, Lohr HR, Crouch RK, Ma JX. Downregulation of cone-specific gene expression and degeneration of cone photoreceptors in the Rpe65$^{-/-}$ mouse at early ages. Invest Ophthalmol Vis Sci 2005; 46:1473-9. [PMID: 15790918].
16. Woodruff ML, Wang Z, Chung HY, Redmond TM, Fain GL, Lem J. Spontaneous activity of opsin apoprotein is a cause of Leber congenital amaurosis. Nat Genet 2003; 35:158-64. [PMID: 14517541].
17. Redmond TM, Yu S, Lee E, Bok D, Hamasaki D, Chen N, Goletz P, Ma J-X, Crouch K, Pfeifer K. Rpe65 is necessary for production of 11-cis-vitamin A in the retinal visual cycle. Nat Genet 1998; 20:344-51. [PMID: 9843205].
18. Seeliger MW, Grimm C, Ståhlberg F, Friedburg C, Jaissle G, Zrenner E, Guo H, Remé CE, Humphries P, Hofmann F, Biel M, Fariss RN, Redmond TM, Wenzel A. New views on RPE65 deficiency: the rod system is the source of vision in a mouse model of Leber congenital amaurosis. Nat Genet 2001; 29:70-4. [PMID: 11528395].
19. Rohrer B, Goletz P, Znoiko S, Ablonczy Z, Ma JX, Redmond TM, Crouch RK. Correlation of regenerable opsin with rod ERG signal in Rpe65−/− mice during development and aging. Invest Ophthalmol Vis Sci 2003; 44:310-5. [PMID: 12506090].
20. Bouillet P, Sapin V, Chazaud C, Messaddeq N, Décimo D, Dollé P, Chambon P. Developmental expression pattern of Stra6, a retinoic acid-responsive gene encoding a new type of membrane protein. Mech Dev 1997; 63:173-86. [PMID: 9203140].
21. Kawaguchi R, Yu J, Honda J, Hu J, Whitelegge J, Ping P, Wiita P, Bok D, Sun H. A membrane receptor for retinol binding protein mediates cellular uptake of vitamin A. Science 2007; 315:820-5. [PMID: 17255476].
22. Blanks JC, Johnson LV, Hageman GS. Stage-specific binding of peanut agglutinin to aggregates of degenerating photoreceptor cells in the rd mouse retina. Exp Eye Res 1993; 57:265-73. [PMID: 8224014].
23. Mieziewska K, van Veen T, Aguirre GD. Structural changes of the interphotoreceptor matrix in an inherited retinal degeneration: a lectin cytochemical study of progressive rod-cone degeneration. Invest Ophthalmol Vis Sci 1993; 34:3056-67. [PMID: 8407213].
24. Landers RA, Rayborn ME, Myers KM, Hollyfield JG. Increased retinal synthesis of heparan sulfate proteoglycan and HNK-1 glycoproteins following photoreceptor degeneration. J Neurochem 1994; 63:737-50. [PMID: 8035198].
25. Kennan A, Aherne A, Palfi A, Humphries M, McKee A, Stitt A, Simpson DAC, Demtroder K, Orntoft T, Ayuso C, Kenna PF, Farrar GJ, Humphries P. Identification of an IMPDH1 mutation in autosomal dominant retinitis pigmentosa (RP10) revealed following comparative microarray analysis of transcripts derived from retinas of wild-type and Rho$^{-/-}$ mice. Hum Mol Genet 2002; 11:547-57. [PMID: 11875049].
26. Hackam AS, Strom R, Liu D, Qian J, Wang C, Otteson D, Gunatilaka T, Farkas RH, Chowers I, Kageyama M, Leveillard T, Sahel JA, Campochiaro PA, Parmigiani G, Zack DJ. Identification of gene expression changes associated with the progression of retinal degeneration in the rd1 mouse. Invest Ophthalmol Vis Sci 2004; 45:2929-42. [PMID: 15326104].
27. Ahuja S, Ahuja P, Caffé AR, Ekstrom P, Abrahamson M, van Veen T. rd1 mouse retina shows imbalance in cellular distribution and levels of TIMP-1/MMP-9, TIMP-2/MMP-2 and sulfated glycosaminoglycans. Ophthalmic Res 2006; 38:125-36. [PMID: 16374054].
28. Lazarus HS, Hageman GS. Xyloside-induced disruption of interphotoreceptor matrix proteoglycans results in retinal detachment. Invest Ophthalmol Vis Sci 1992; 33:364-76. [PMID: 1740367].
29. Bandah-Rozenfeld D, Collin RW, Banin E, van den Born LI, Coene KL, Siemiatkowska AM, Zelinger L, Khan MI, Lefeber DJ, Erdinest I, Testa F, Simonelli F, Voesenek K, Blokland EA, Strom TM, Klaver CC, Qamar R, Banfi S, Cremers FP, Sharon D, den Hollander AI. Mutations in IMPG2, encoding interphotoreceptor matrix proteoglycan 2, cause autosomal-recessive retinitis pigmentosa. Am J Hum Genet 2010; 87:199-208. [PMID: 20673862].
30. Yue BY, Kawa JE, Chang IL, Sawaguchi S, Fishman GA. Effects of chondroitin sulfate on cultured human retinal pigment epithelial cells. Cell Biol Int Rep 1991; 15:365-76. [PMID: 1913846].
31. Inatani M, Tanihara H. Proteoglycans in retina. Prog Retin Eye Res 2002; 21:429-47. [PMID: 12207944].

Articles are provided courtesy of Emory University and the Zhongshan Ophthalmic Center, Sun Yat-sen University, P.R. China. The print version of this article was created on 16 November 2013. This reflects all typographical corrections and errata to the article through that date. Details of any changes may be found in the online version of the article.